

K and L x rays induced by 5-MeV/amu α -particle and nitrogen-ion bombardment of ten target elements ranging from Cr to Bi

Yohko Awaya, Koichi Izumo, Tatsuji Hamada, Masaharu Okano, Tan Takahashi,
A. Hashizume, Yoshihiko Tendow, and Takeo Katou

The Institute of Physical and Chemical Research, Wako-shi, Saitama, 351 Japan

(Received 14 May 1975)

The K and L x rays from ten target elements from Cr to Bi bombarded by 5-MeV/amu α particles and N ions were measured by a Si(Li) detector. Energy shifts of K x rays and intensity ratios of $K\beta/K\alpha$, $L\alpha/LI$, $L\alpha/L\beta$, $L\alpha/L\gamma$, and L/K were determined by analyzing the experimental results. The ratio of the reduced K-shell ionization cross sections, R_{2K} , showed a systematic deviation from the Z_1^2 dependence.

I. INTRODUCTION

In recent years, many studies have been made of the x rays induced by heavy-ion bombardments. Two kinds of excitation mechanisms of the inner-shell electrons have been discussed and applied to interpret experimental results. One is the electron promotion caused by the formation of quasi-molecular orbitals during the collision time, and the other is the direct Coulomb excitation between the projectile and the bound electron.

The former prevails for the case of $Z_1 \approx Z_2$ and $v_1 < v_2$ where Z_1 and Z_2 are the atomic numbers of the projectile and the target atom and v_1 and v_2 are the velocities of the projectile and of the bound electron to be excited, respectively. The electron promotion model¹ has explained the large cross section for creating the inner-shell vacancy under these conditions. Many experimentally observed phenomena, such as the level-matching effect and molecular-orbital x rays, have been interpreted with this mechanism.

The latter dominates when v_1 is so high that the projectile is deemed to be a bare nucleus or when the condition of $Z_1 \ll Z_2$ holds even though v_1 is not so high. The plane-wave Born approximation² (PWBA) and the binary-encounter approximation³ (BEA) have been applied mainly for this case, in which the cross section for creating the K-shell vacancy is represented universally by using reduced parameters. Both approximation methods predict a Z_1^2 dependence of the cross section; the prediction has been compared with extensive experimental work done with light projectiles ($Z_1 \leq 2$).⁴ Detailed studies,⁵⁻⁸ however, have shown deviation of the cross section from the Z_1^2 dependence, which can be attributed to a Z_1^3 -dependent term in addition to the Z_1^2 -dependent part.

In the case where the swift heavy ions are used as projectiles and $Z_1 \ll Z_2$, however, experimental data are not so abundant. Saltmarsh *et al.*⁹ have studied the energy shift of K x rays and $K\beta/K\alpha$

intensity ratios by bombarding Ti, Fe, Co, Zr, and Sn targets with 5-MeV/amu He, C, O, and Ne and 10-MeV/amu C ions and suggested that the Coulomb excitation mechanism is applicable to the explanation of experimental results. Van der Woude *et al.*¹⁰ and Cue *et al.*¹¹ have deduced the existence of a Z_1^3 dependence for 5- and 7.1-MeV/amu heavy ions, respectively. Li and Watson¹² have measured the $K\beta/K\alpha$ intensity ratios of K x rays emitted from targets of $19 \leq Z_2 \leq 47$ following ionization by deuterons, α particles, and C ions.

The aim of the present work is twofold. The first is to obtain more systematic information about the mechanism of vacancy formation in inner shells by bombarding ten target elements ranging from Cr to Bi with 5-MeV/amu α particles and N ions. The energy shift of K x rays and the deviation from the Z_1^2 dependence of the cross section have been studied for this purpose. The amount of deviation from the Z_1^2 dependence has been plotted against a reduced parameter that includes characteristic quantities of projectiles and target atoms. The second is to provide additional K- and L-x-ray data induced by heavy-ion impact, especially for the elements heavier than $Z_2 \approx 50$, since in this mass region data are less available than in lighter elements. The preliminary results of this work have been reported.¹³

II. EXPERIMENTAL METHOD

Beams of α particles and N^{4+} ions accelerated by the cyclotron of the Institute of Physical and Chemical Research were led to a target chamber whose section perpendicular to the beams was square. The frame of the target chamber and the target holder were made of aluminum and the four walls parallel to the beams were made of Lucite plates to reduce the x-ray background at a detector. The incident energy of both projectiles was 5 MeV/amu. A target was placed at an inclination

of 45° with respect to the beam and the detector. The x rays from the target induced by the beam bombardment were detected by a Si(Li) x-ray detector which was placed perpendicular to the beam direction. The energy resolution of the detector was 270 eV (full width at half-maximum) at 6.4 keV. Between the target and the detector, there were two 50- μ m Be foils, i.e., the windows of the target chamber and the detector, in addition to an air space of about 7 mm.

The relative efficiency of the detector was determined with the same source-detector arrangement by using x and γ rays from radioisotopes ^{54}Mn , ^{57}Co , ^{65}Zn , ^{109}Cd , ^{137}Cs , ^{203}Hg , and ^{241}Am . The effects on the efficiency of the experimental conditions were thus taken into account.

Target elements studied were ^{24}Cr , ^{26}Fe , ^{29}Cu , ^{38}Sr , ^{47}Ag , ^{56}Ba , ^{142}Nd , ^{71}Lu , ^{82}Pb , and ^{83}Bi . These target elements were chosen from the following three points of view: (i) They were appropriately distributed in the periodic table. (ii) Each of them has a corresponding, easily available radionuclide which emits the same characteristic x rays for use as the energy standard for measuring the energy shift. (iii) We have paid attention to the existence of excited state in the target nuclei, which decays with a large conversion coefficient because the energy of the projectile was high enough to induce nuclear events. Such an excited state can be fed not only through the Coulomb excitation but also through the decay chain of produced radioactivities by (α, xn) or (N, xn) reactions. This contribution becomes important for the targets with higher atomic number as the K -vacancy production cross section decreases with target atomic number. For this sake, it is desirable that the energy of the first excited state of the target nucleus is high and the lives of the induced radioactivities are as long as possible. The isotopically enriched target of Nd was used for this reason. To check the contribution of the nuclear Coulomb excitation and nuclear transition, γ -ray spectra were measured by using a Ge(Li) detector but their contribution could be neglected except for Lu. The energy of the first excited state of ^{175}Lu is so low that the γ transition from this to the ground state was observed as well as x rays. The contribution of this nuclear transition was subtracted from the yield of K x rays.

The targets of Cr, Fe, Cu, Ag, Pb, and Bi were prepared by evaporating these metallic elements on the backing, while the others were made by sedimentation of their insoluble compounds. Mylar films of 4- μ m thickness were used as the backing except for Ag. A thinner Formvar film was used for Ag, since the x-ray spectrum obtained by bombarding a Mylar film had a hump in

the vicinity of the position of Ag L x rays which would originate in the impurity elements in the film. Thickness of the target materials ranged from about 20 $\mu\text{g}/\text{cm}^2$ for Cr to 350 $\mu\text{g}/\text{cm}^2$ for Bi.

During the measurement of x rays, the counting rate was kept below 300 sec^{-1} in order to reduce the pileup effect. The number of projectiles was determined from a measurement of the integrated beam current by a combination of a picoammeter and a current integrator and a value for an effective charge of projectiles. By referring to the work on the charge exchange for N^{4+} ions¹⁴ and considering the target thickness, the charge distribution was considered to be in equilibrium. Thus the value¹⁵ of 6.9 was taken for the effective charge of N ions at the Faraday cup.

For N ions, the energy shift of x rays was observed and, for some target elements, the energy of some $K\beta_2$ satellites became higher than the K absorption edge. For L x rays, the energies of some components are larger than the L_3 or L_2 absorption edge in nature. In order to estimate the amount of absorption in the target, the yield of x rays was measured with and without inserting between the two Be windows a spare target whose thickness was almost the same as the target to be bombarded. As the amount of the absorption was found to be smaller than 2%, the correction for this effect was omitted. For measurements of K x rays from elements heavier than Ag, some absorbers were inserted between the two Be windows to reduce the L x rays. A correction was made for the absorption of K x rays by these absorbers.

III. RESULTS AND DISCUSSION

A. Spectrum

In the low-energy region of x-ray spectra a continuous energy distribution of photons was always observed as a background. From the pattern of the spectra and the dependence on the incident energy, this was found to be due to the bremsstrahlung from recoil electrons (δ rays) created by the projectiles within the target.¹⁶ For protons, a precise study has been made by Folkmann *et al.*¹⁷ Examples of this spectrum are shown in Fig. 1 together with the calculated curve fit to the experimental data. The position of the estimated end-point energy, $\sim 2.2E_0$ keV, is shown by an arrow, where E_0 (in MeV) is the incident-particle energy per nucleon.

The peak position and the peak area of the characteristic x rays were determined by using a χ^2 fit, assuming the shape of a peak to be Gaussian. The pattern of the background under the peak was usually assumed to be linear with the channel

number. An exponential background, however, was assumed for some L x rays, since their background was attributed to the bremsstrahlung described above and was estimated from background counts in two energy regions several keV apart. Unresolved peaks were also separated by the same method. In the case of L x rays, which consist of many components, the peak separation was made by referring to transition probabilities¹⁸ and tables of x-ray energies.¹⁹

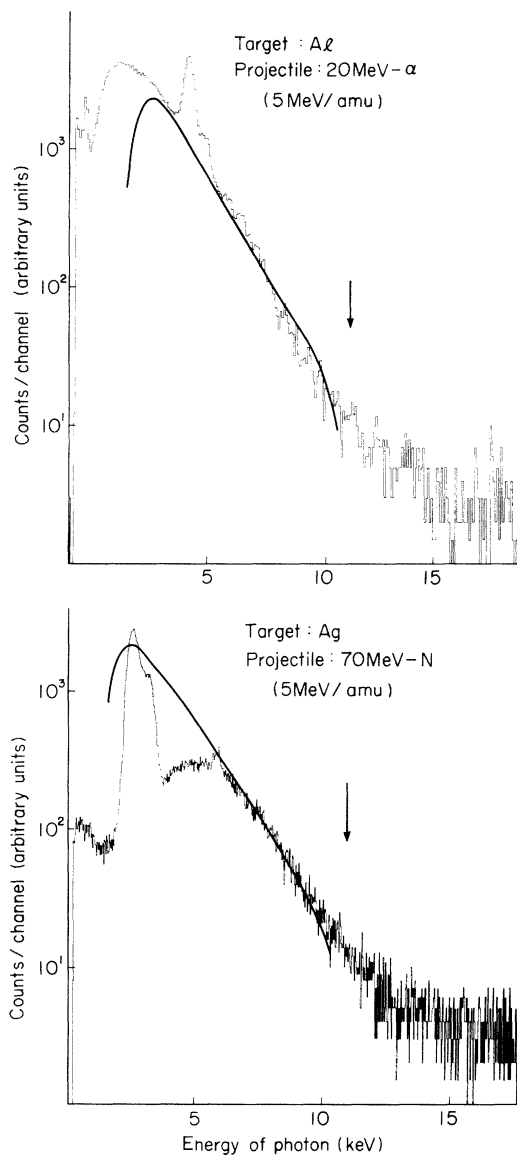


FIG. 1. X-ray spectra obtained for α -particle and N-ion bombardment, showing the continuous background in the low-energy region. Experimental conditions are indicated in each figure. The arrows mark the position of end-point energy by our estimation.

Typical spectra of K and L x rays observed for α -particle and N-ion bombardments and those from the corresponding radioisotopes are shown in Figs. 2 and 3.

Error bars in Figs. 2–9 and errors in Tables I and II include errors in the counting statistics, in the background subtraction, in the relative counting efficiency and energy calibration of the detector, and in fitting the peak to a Gaussian curve.

B. Energy shift

The energy shift of characteristic x rays induced by heavy-ion impact has been reported by many authors since Richard *et al.*²⁰ studied the energy shift of the $K\beta$ lines of Cu and Ni. The origin of the shift has been attributed to the multiple excitation of inner-shell electrons.^{21,22} The amount of the K -x-ray energy shift seems to depend on the cross section for the creation of L vacancies. By the prediction of the PWBA or BEA, this cross section will take a maximum value under the condition $E/\lambda u_L \approx 1$, where E is the energy

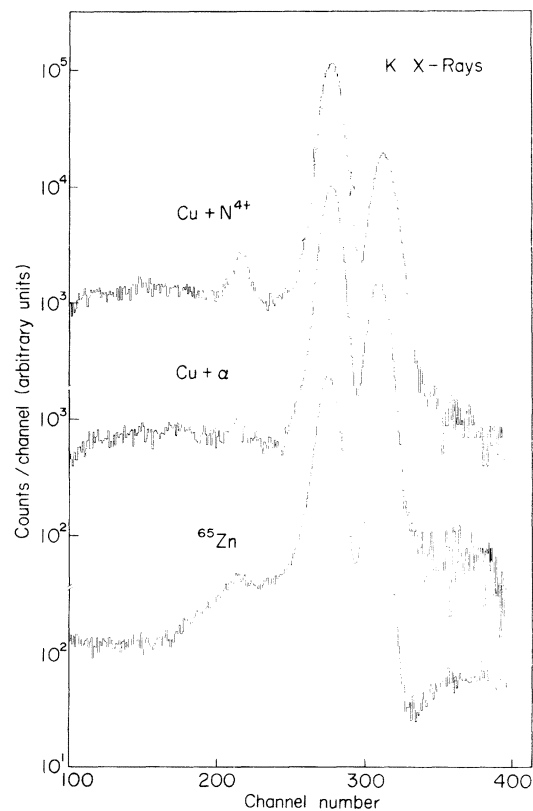


FIG. 2. Spectra of K x rays obtained by N-ion and α -particle bombardment of the Cu target and by the decay of ^{65}Zn .

of the projectile, λ is the ratio of projectile mass (m_1) to the electron mass (m_e), and u_L is the average binding energy of target L electrons. Saltmarsh *et al.*⁹ have studied this effect by measuring the Ti and Fe K -x-ray energy shift as a function of the bombarding energy of O ions. They plotted the $K\alpha$ and $K\beta$ energy shift against $E/\lambda u_L$ for Fe and Ti targets, respectively, and found that the maximum occurs at $E/\lambda u_L \approx 1.3$.

Similar plots were made for the present data and the results are shown in Fig. 4. In the present case, u_L was varied while E was kept constant. The amount of the energy shift of x rays was estimated by comparing the peak position in the spectra obtained for the particle-excited target with that for the corresponding radioisotopes of ^{54}Mn , ^{57}Co , ^{65}Zn , ^{88}Y , ^{109}Cd , ^{137}Cs , $^{143,144}\text{Pm}$, ^{175}Hf , and ^{207}Bi . When they decay by the electron-capture process or when the excited states of their daughter nuclei decay by the internal conversion process, they emit the same characteristic x rays as those from the corresponding target elements.

The amount of $K\alpha$ energy shift increases until $E/\lambda u_L$ rises to about 1.3 and after that becomes almost constant. When the $K\alpha_1$ and $K\alpha_2$ lines could be separated, their shifts were found to be

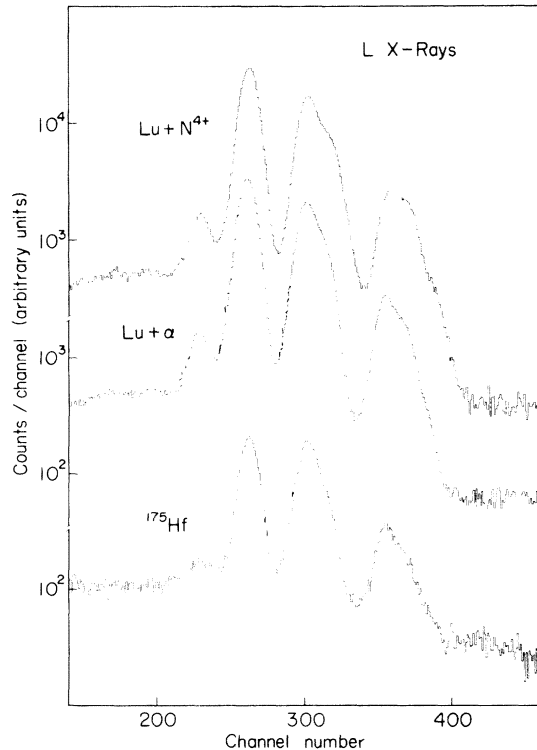


FIG. 3. Spectra of L x rays obtained N-ion and α -particle bombardment of the Lu target and by the decay of ^{175}Hf .

almost the same. The shift of $K\beta_1$ x rays has a maximum at $E/\lambda u_L \approx 1.2$. The value of $E/\lambda u_L$ where the amount of $K\alpha$ and $K\beta_1$ energy shifts has a maximum in the present result agrees very well with that of Saltmarsh *et al.* even though the variable quantity in the parameter $E/\lambda u_L$ is different in these two works.

The amount of the energy shift of $K\beta_2$ x rays was plotted as a function of $E/\lambda u_M$, where u_M is the average binding energy of M -shell electrons, instead of a function of $E/\lambda u_L$. If one wants to plot this value against $E/\lambda u_L$ one should refer to the element symbol shown in the figures. Then the maximum of the shift of $K\beta_2$ line, which is found at $E/\lambda u_M \approx 3$, is displaced to $E/\lambda u_L \approx 0.5$. On the contrary, when the values of $K\beta_1$ energy shift are plotted as a function of $E/\lambda u_M$ the maximum will be found at $E/\lambda u_M \approx 13$.

These effects may be explained qualitatively as follows: When we consider an electron in a specified shell, its binding energy is affected more

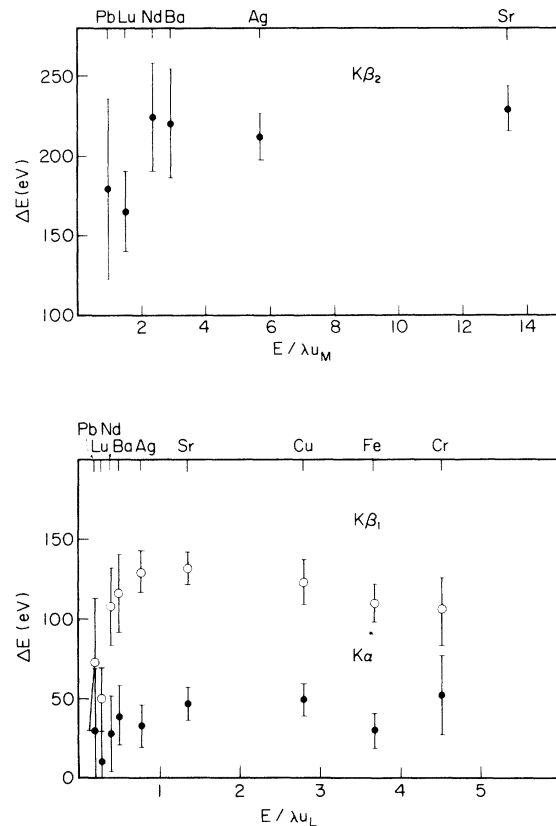


FIG. 4. Energy shift of $K\alpha$, $K\beta_1$, and $K\beta_2$ x rays for N-ion bombardment. The name of the target element corresponding to each experimental point is also shown. The transformation of the abscissa from $E/\lambda u_L$ to $E/\lambda u_M$, or vice versa, can be made by referring to the element symbols.

strongly by the vacancies in inner shells than by those in outer shells. Hence the vacancies in the L shell show a more marked effect on the shift of $K\beta_1$ lines than on that of $K\alpha$ lines and the definite maximum is seen in the $K\beta_1$ energy shift. The vacancies in the M shell also contribute to the shift of these x rays, but their contribution is rather masked by the effect of L vacancies.

For the shift of $K\beta_2$ x rays, the vacancies in the M shell play a more important role than for those of $K\beta_1$ and $K\alpha$ x rays, since $K\beta_2$ x rays are emitted by the transition from the N shell to the K shell. The amount of the energy shift which originates in the M -shell vacancies would have a maximum at $E/\lambda u_M \approx 1$. The maximum, however, is seen at $E/\lambda u_M \approx 3$, and this difference is considered to be caused mainly by the additive vacancies in the L shell.

C. Intensity ratios of x-ray components

It has been found that the $K\beta/K\alpha$ intensity ratios observed for heavy-ion bombardments were different from those for photoionization, electron bombardment, and radioisotope decay. The cause

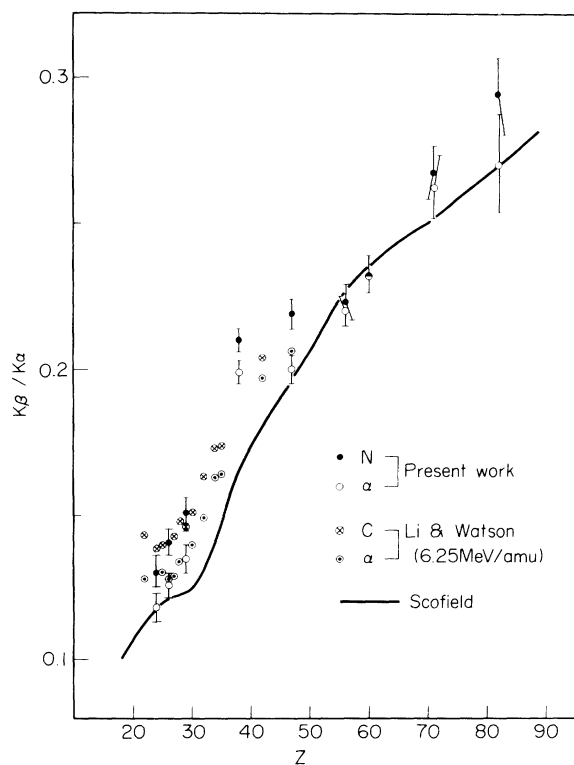


FIG. 5. $K\beta/K\alpha$ values obtained by N-ion and α -particle bombardment. The data for 6.25-MeV/amu α -particle and C-ion impact (Ref. 12) and the calculated curve by Scofield (Ref. 18) are also shown for comparison.

TABLE I. $K\alpha/K\beta$ intensity ratios for K x rays induced by 5-MeV/amu α particles and N ions.

Target element	α particles	N ions
^{24}Cr	0.118 ± 0.004	0.131 ± 0.005
^{26}Fe	0.126 ± 0.003	0.141 ± 0.004
^{29}Cu	0.135 ± 0.005	0.151 ± 0.005
^{38}Sr	0.199 ± 0.004	0.210 ± 0.004
^{47}Ag	0.200 ± 0.005	0.223 ± 0.005
^{56}Ba	0.220 ± 0.004	0.223 ± 0.006
^{60}Nd	0.232 ± 0.006	0.232 ± 0.007
^{71}Lu	0.262 ± 0.011	0.267 ± 0.009
^{82}Pb	0.270 ± 0.017	0.294 ± 0.013

of this difference has been attributed to the multiple ionization.²¹⁻²³ Recently, Li and Watson¹² measured the $K\beta/K\alpha$ intensity ratio for the elements between K and Ag using 2.35–12.5-MeV/amu deuterons, α particles, and N ions. They also studied the variation of $K\beta/K\alpha$ with electronic configurations of L and M shells.

The $K\beta/K\alpha$ ratio obtained in this work is shown in Fig. 5, and the values are listed in Table I. For comparison the figure includes the data obtained by Li and Watson for 6.25-MeV/amu α particles and C ions and the curve calculated by Scofield.¹⁸ The present data seem to agree well with the data obtained by Li and Watson, within the limit of error. The ratio of $K\beta/K\alpha$ for N ions and α particles, $(K\beta/K\alpha)_N/(K\beta/K\alpha)_\alpha$, is larger than unity, as shown in Fig. 6, and this also agrees with the results obtained by Li and Watson.

It was difficult to obtain precise intensity ratios of L -x-ray components, such as $L\alpha_1/L\alpha_2$ or $L\beta_{2+15}/L\alpha_1$, because of the insufficient energy resolution. We obtained the values of $L\alpha/L\beta$, $L\alpha/L\gamma$, and $L\alpha/L\gamma$ ratios. When the intensities of $L\beta$ and $L\gamma$ x rays were estimated, the $L\beta$ and $L\gamma$ lines were separated into a few main components by the χ^2 -fitting method as described above and each peak area was corrected by using the detection efficiency for each peak energy. The

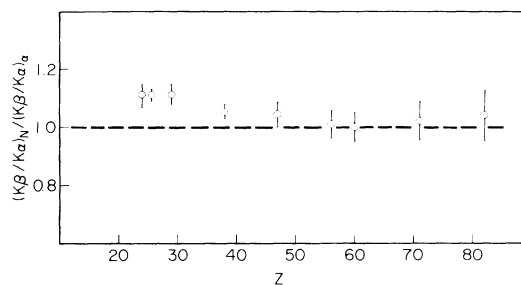


FIG. 6. Ratio of $K\beta/K\alpha$ for N-ion and α -particle bombardment.

results are shown in Fig. 7 in comparison with calculated curves. The solid curve for the $L\alpha/L\beta$ ratio is the value calculated by Scofield.¹⁸ The dashed curves for the $L\alpha/L\beta$ and $L\alpha/L\gamma$ ratios were obtained in the following way: Intensity ratio of two x rays is expressed as (intensity ratio) = (ratio of vacancy-production probabilities) \times (ratio of transition probabilities) \times (ratio of fluorescence yields). The term of the ratio of transition probabilities is calculated using the results by Scofield. In calculating the ratios, the same fluorescence yield and ionization cross section of an orbital electron were taken for each transition contributing to a given line intensity. Then the term for the ratio of fluorescence yields can be eliminated and the term for the vacancy-production probabilities can be represented by the ratio of the numbers of electrons in the lower

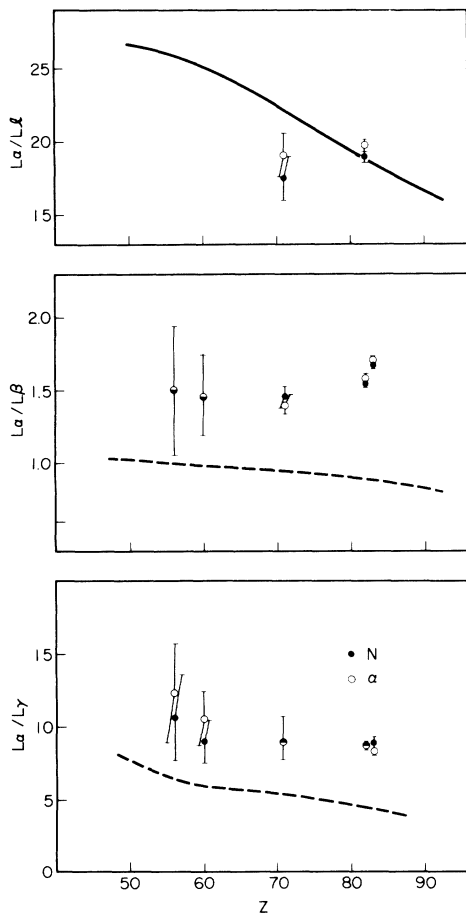


FIG. 7. $L\alpha/L\beta$, $L\alpha/L\gamma$, and $L\alpha/L\gamma$ values obtained by α -particle and N-ion bombardment. The solid curve for $L\alpha/L\beta$ calculated by Scofield (Ref. 18) is also shown. The dashed curves for $L\alpha/L\beta$ and $L\alpha/L\gamma$ are those estimated on the basis of the calculation done by Scofield.

orbits where vacancies will be produced.

As is seen in Fig. 7, the experimental values for α -particle and N-ion impact are the same for all target elements within the limits of uncertainty. From this fact it might be deduced that in the outer shells α particles and N ions give similar effects on ionization. The calculated values for $L\alpha/L\beta$ and $L\alpha/L\gamma$, on the other hand, are about one-half of the experimental values for both ratios throughout the region of atomic numbers of the targets employed. But the variations with atomic number are systematically parallel for the calculated and experimental ratios. Therefore the discrepancy between the two values of the ratio could be attributed to the difference between the ionization cross section of L_3 electrons ($L\alpha$ x rays originate from the transition to the L_3 hole) and that of L_2 electrons (main components of $L\beta$ and $L\gamma$ x rays originate in the transition to the L_2 hole).

The ratios of K- and L-x-ray yields for α -particle and N-ion bombardment are shown in Fig. 8. The difference between the two ratios increases as the atomic number of the target atom decreases. The L-x-ray yield relative to that of K x rays for N-ion bombardment is about a factor of 2 larger than that for α -particle bombardment. This may be due to the change of the fluorescence yield and the effect of polarization of orbital electrons.

D. Z_1^2 dependence

The PWBA predicts the Z_1^2 dependence of ionization cross section, that is, in the case of K-shell ionization

$$R_{2K} \equiv \frac{\sigma_{2K}(Z_1')/Z_1'^2}{\sigma_{2K}(Z_1)/Z_1^2} = 1$$

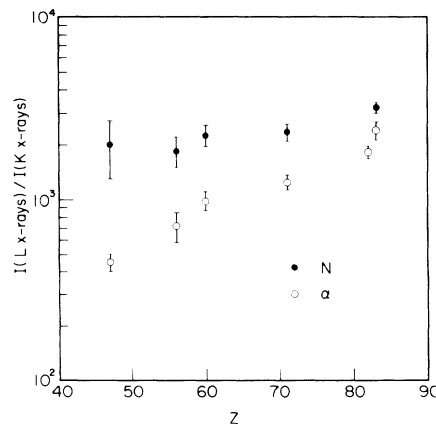


FIG. 8. Intensity ratio of K and L x rays obtained by N-ion and α -particle bombardment.

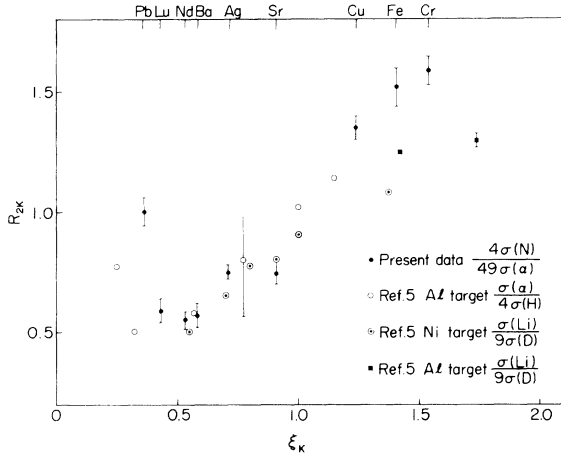


FIG. 9. Ratios R_{2K} of K -shell ionization cross sections as a function of ξ_K . The name of the target element corresponding to each experimental point in the present work is also shown. The results obtained by Basbas *et al.* (Ref. 5) are shown for comparison. Though their data have many more points, some of them are neglected as the points show a smooth curve. The abscissa of their data is converted from v_1/v_{2K} to ξ_K by reading the values of $\frac{1}{2}\theta$ from their figure.

if the incident projectile energies per nucleon are the same, where $\sigma_{2K}(Z_1)$ is the K -shell ionization cross section of the target atom of atomic number Z_2 for the incident charged particle of atomic number Z_1 . Some experimental studies, however, showed the deviation from the Z_1^2 dependence in the K -shell ionization cross sections.^{5-8,10,11} The cause of this deviation would be twofold, i.e., the increase of binding energy of target electrons (prevailing at $v_1 < v_{2K}$) and the polarization of them (prevailing at $v_1 \geq v_{2K}$), where v_{2K} is the velocity of a K electron of a target atom ($v_{2K} = Z_{2\text{eff}} e^2 / \hbar$, $Z_{2\text{eff}} = Z_2 - 0.3$). These two effects show a Z_1^3 dependence and give contributions with opposite signs to the cross section. They cancel each other, giving a ratio R_{2K} of unity, at $v_1/v_{2K} = \frac{1}{2}\theta_K$, or $\xi_K = v_1 / (\frac{1}{2}\theta_K v_{2K}) = 1$, where $\theta_K = 2I_{2K}/Z_{2\text{eff}}^2$ and I_{2K} (in a.u.) is the ionization energy of a K -shell electron.

The Z_1^3 dependence has been studied precisely for light-particle impact. As to heavy-ion impact, Van der Woude *et al.*¹⁰ have suggested this dependence in their experiments with 5-MeV/amu α -particle and C-, O-, and Ne-ion bombardment. Cue *et al.*¹¹ studied this contribution for 7.1-MeV/amu α -particle and B-, C-, N-, O-, F-, and Ne-ion bombardment on Cd, Y, Fe, and Ca. The former plotted R_{2K} vs $E/\lambda u_K$ and found that R_{2K} crosses unity at $E/\lambda u_K \approx 0.25$. The latter analyzed their results for R_{2K} for each target element and concluded that their results are explicit

TABLE II. Values of ξ_K and R_{2K} . $\xi_K = v_1 / \frac{1}{2}\theta_K v_{2K}$, $\theta_K = 2I_{2K}/Z_{2\text{eff}}^2$, $v_{2K} = Z_{2\text{eff}} e^2 / \hbar$, $Z_{2\text{eff}} = Z_2 - 0.3$, and $R_{2K} = 4\sigma(N)/49\sigma(\alpha)$.

Target element	ξ_K	R_{2K}
²⁴ Cr	1.56	1.59 ± 0.05
²⁶ Fe	1.42	1.52 ± 0.08
²⁹ Cu	1.26	1.35 ± 0.05
³⁸ Sr	0.92	0.74 ± 0.04
⁴⁷ Ag	0.71	0.75 ± 0.03
⁵⁶ Ba	0.58	0.57 ± 0.05
⁶⁰ Nd	0.53	0.55 ± 0.03
⁷¹ Lu	0.43	0.61 ± 0.05
⁸² Pb	0.36	1.03 ± 0.06

evidence for the existence of a Z_1^3 -dependent term and that the two competing effects mentioned above cancel each other at $\xi_K = 1.04$, i.e., for the Y target.

The result of the present work is shown in Fig. 9. The data of Basbas *et al.*⁵ for protons, deuterons, and Li ions as projectiles have been adapted to Fig. 9 for comparison by converting the parameter v_1/v_{2K} to ξ_K by graphical reading. Their data include many more points than plotted in Fig. 9, where only typical points are referred to. Numerical values of the present data are listed in Table II.

Values of R_{2K} are plotted as a function of ξ_K because contributions of the two above-mentioned effects on R_{2K} depends on the parameter ξ_K as a whole, not individually on Z_2 , v_{2K} , and v_1 . The fluorescence yield ω_K for N-ion impact is assumed to be the same as for α -particle bombardment. The ω_K increases in the case where multiple excitation occurs, but this effect is not considered to be very large in the present case. The dependence of R_{2K} on ξ_K is very similar for both data, especially for $\xi_K < 1$, and shows a clear deviation from Z_1^2 dependence of the ionization cross section. As is seen in Fig. 9, the two effects cancel at $\xi_K \approx 1$, which is consistent with the results of Cue *et al.* and Van der Woude *et al.* cited above, where the value of $E/\lambda u_L \approx 0.25$ corresponds to the value of $\xi_K \approx 1.2$. For the elements corresponding to $\xi_K > 1$, that is, Cr, Fe, and Cu, the change of ω_K for N-ion impact may be greater than that for the heavier elements. In addition to the effect of polarization, some amount of the deviation might be due to this factor.

The points at $\xi_K < 0.5$ deviate from the line which means the existence of the Z_1^3 -dependent term. This deviation has been explained by the deflection of the projectile by the target nuclei. For the target elements with large Z_2 , relativistic effects on the bound electron may be included in the present

data but this effect cannot be separated from others.

IV. SUMMARY

The energy-shift measurements for $K\alpha$, $K\beta_1$, and $K\beta_2$ x rays have shown the effect of the L - and M -shell vacancies predicted by the BEA. The deviation from the Z_1^2 dependence observed for light projectiles, which shows the existence of the Z_1^3 -dependent term, has been obtained in

the present work. On the basis of these results, the inner-shell ionization caused by N-ion bombardment under the present experimental conditions (incident energy and target elements) is considered to be caused mainly by direct Coulomb excitation.

Our data are concerned with targets with higher atomic number and rather-high-energy projectiles. As such data have not been abundant, they would contribute to the systematics of the inner-shell ionization process by heavy ions.

-
- ¹U. Fano and W. Lichten, *Phys. Rev. Lett.* **14**, 627 (1965); W. Lichten, *Phys. Rev.* **164**, 131 (1967).
²E. Merzbacher and H. W. Lewis, *Handb. Phys.* **34**, 166 (1958).
³J. D. Garcia, *Phys. Rev. A* **1**, 280 (1970); **4**, 955 (1971).
⁴J. D. Garcia, R. J. Fortner, and T. M. Kavanagh, *Rev. Mod. Phys.* **45**, 111 (1973), and references cited therein.
⁵G. Basbas, W. Brandt, R. Laubert, A. Ratkowski, and A. Schwarzschild, *Phys. Rev. Lett.* **27**, 171 (1971).
⁶C. W. Lewis, J. B. Natowitz, and R. L. Watson, *Phys. Rev. Lett.* **26**, 481 (1971); *Phys. Rev. A* **5**, 1773 (1972).
⁷G. Basbas, W. Brandt, and R. Laubert, *Phys. Rev. A* **7**, 983 (1973).
⁸N. Stolterfoht, D. Schneider, and K. G. Harrison, *Phys. Rev. A* **8**, 2363 (1973); N. Stolterfoht and D. Schneider, *Phys. Rev. A* **11**, 721 (1975).
⁹M. J. Saltmarsh, A. van der Woude, and C. A. Ludemann, *Phys. Rev. Lett.* **29**, 329 (1972).
¹⁰A. van der Woude, M. J. Saltmarsh, C. A. Ludemann, R. L. Hahn, and E. Eichler, in *Proceedings of the International Conference on Inner Shell Ionization Phenomena and Future Applications, Atlanta, Georgia, 1972*, edited by R. W. Fink, S. T. Manson, J. M. Palms, and P. V. Rao, CONF-720 404 (U. S. Atomic Energy Commission, Oak Ridge, Tenn., 1973), p. 1388.
¹¹N. Cue, V. Dutkiewicz, P. Sen, and H. Bakhru, *Phys. Rev. Lett.* **32**, 1155 (1974).
¹²T. K. Li and R. L. Watson, *Phys. Rev. A* **9**, 1574 (1974).
¹³Y. Awaya, T. Hamada, M. Okano, A. Hashizume, T. Takahashi, K. Izumo, Y. Tendow, and T. Katou, *IPCR Cyclotron Progress Report 7*, 87 (1973) (unpublished).
¹⁴Tadao Tonuma, Isao Kohno, Yoshitoshi Miyazawa, Fusaiko Yoshida, Takashi Karasawa, Tan Takahashi, and Satoru Konno, *J. Phys. Soc. Jpn.* **34**, 148 (1973).
¹⁵A. B. Wittkower and H. D. Betz, *At. Data* **5**, 113 (1973).
¹⁶K. Izumo, Y. Tendow, Y. Awaya, T. Katou, M. Okano, A. Hashizume, T. Takahashi, and T. Hamada, in Ref. 13, p. 93.
¹⁷F. Folkmann, C. Garrde, T. Huus and K. Kemp, *Nucl. Instrum. Meth.* **116**, 487 (1974).
¹⁸J. H. Scofield, *Phys. Rev.* **179**, 9 (1969); *Phys. Rev. A* **10**, 1507 (1974); *At. Data Nucl. Tables* **14**, 121 (1974).
¹⁹J. A. Bearden, *Rev. Mod. Phys.* **39**, 78 (1967).
²⁰P. Richard, I. L. Morgan, T. Furuta, and D. Burch, *Phys. Rev. Lett.* **23**, 1009 (1969).
²¹D. Burch and P. Richard, *Phys. Rev. Lett.* **25**, 983 (1970).
²²A. R. Kundson, D. J. Nagel, P. G. Burkhalter, and K. L. Dunning, *Phys. Rev. Lett.* **26**, 1149 (1971).
²³R. L. Watson and T. K. Li, *Phys. Rev. A* **4**, 132 (1971).